

Nov 13th, 12:00 AM

# Criteria for Connection Spacing in Cold-formed Steel

Muzaffer Yener

Seventh International Specialty Conference on Cold-Formed Steel Structures
St. Louis, Missouri, U.S.A., November 13-14, 1984

# CRITERIA FOR CONNECTION SPACING IN COLD-FORMED STEEL

By Muzaffer Yener[1]

M.ASCE

## INTRODUCTION

A great variety of cold-formed steel shapes is often used in combination with cover plates, as illustrated in Fig. 1, to form closed cellular panels. These sections are generally used for resisting loads acting perpendicular to their surfaces. In this paper, the spacing requirements of connectors that are used to fasten the cover plate to the fluted sheet to resist gravity loads are investigated. Comparisons with test results are made, and an illustrative example is presented in an appendix.

It is of economical importance to design such composite sections so that the cover plate can be considered as an integrated, load-carrying component of the assembly. Regardless of the type of fastener used, in a well-designed panel the spacing of connections should be such that the flexural strength of the assembly predicted on the basis of the full composite behavior is developed. In thin-walled compression elements, the maximum allowable spacing of connections is governed either by the allowable strength of the connection, or by separation of component compression plates along the lines of connections.

1 Assistant Professor, School of Civil Engineering, Purdue University, West Lafayette, IN.

The allowable shear loads in mechanical fasteners vary widely depending on the type of fastener and on details of the assembly, such as the thickness and texture of the surfaces being joined. In addition to mechanical fasteners, such as bolts, rivets, and screws, spot welds are utilized as a means of connecting light-gage steel component parts. The present AISI Specification (3) contains detailed provisions only for welded and bolted connections.

## REVIEW OF CURRENT DESIGN PHILOSOPHY

The primary function of fasteners in cold-formed steel roof decks and floor panels is to resist shear stresses produced by flexural loading. Allowable shear force per spot in sheets joined by spot welding, along with shear stress and allowable bearing stress for bolted connections, based on safety factors in excess of 2.0, are given in the AISI Specification. For fasteners not covered by the Specification, the allowable connection strength is to be determined on the basis of data obtained from tests conducted on specimens representative of the actual assembly, using an appropriate safety factor.

In the present AISI Specification, the maximum spacing of welds to prevent cylindrical buckling of compression elements is determined as follows: the strip of the compressed plate between two adjacent spot welds is assumed to act as a column of length s (5), which is the center-to-center distance between welds as shown in Fig. 2. Then, the strip is analyzed as a fixed ended

column by conservatively basing the effective length kl on 0.6s in the Euler buckling formula, $\sigma_e = \pi^2 E/(kl/r)^2$. The limiting value of s for the prevention of column-type buckling of the strip prior to yielding is then found by substituting the yield stress $\sigma_y$ for $\sigma_e$ in this equation. The radius of gyration of the strip column, $r = t/\sqrt{12}$, is computed in Fig. 3. In addition to the values above, using E = 29,500 ksi (203,400 MPa) in the Euler buckling equation gives

$$s = \frac{259t}{\sqrt{\sigma_y}} \qquad (1)$$

where t is the thickness in inches of the compression flange. If a safety factor of 1.67 against yielding is incorporated, Eq. 1 can be expressed in terms of the basic design stress, $f = 0.60\sigma_y$. As a result, the maximum allowable spacing of welded connections in compression elements is given in Section 4.4(b) of the present AISI Specifications as $200t/\sqrt{f}$.

This provision is similar to that adopted by the aircraft industry for corresponding situations. The overly conservative nature of this requirement, as applied to cold-formed steel flexural panels, has been experimentally verified (4,6,9).

In order to develop the full flexural capacity of cold-formed steel composite members, additional consideration must be given to the local buckling of unstiffened compression elements. For this reason, the AISI Specification requires that connection spacing should not exceed three times the flat-width of the narrowest unstiffened compression element of the assembly, with

appropriate lower bounds on s. An unstiffened compression element is one which is adequately supported along only one of its longitudinal edges.

## EVALUATION OF CURRENT PHILOSOPHY

If the fasteners are closely spaced as illustrated in Fig. 4, the flat plate will behave as a stiffened compression element having a width w equal to the transverse distance between the lines of connections. It should be emphasized that regardless of how closely the connections are spaced, the buckling of the cover sheet as a plate may not be prevented. Depending primarily on the rotational restraint provided by fasteners and on the width-to-thickness ratio, w/t, the cover plate may buckle at a critical stress, $\sigma_{cr}$, less than the yield stress, $\sigma_y$. If the separation of compressed plates is prevented, the maximum flexural capacity of such a composite panel will be obtained when the unloaded compression edge stress along the lines of connections, $\sigma_c$, becomes equal to $\sigma_y$. The implication of the spacing given by Eq. 1 is that, as $\sigma_c$ increases from $\sigma_{cr}$ to $\sigma_y$, the column-type buckling of the strip plate between adjacent connections would not take place. This in turn would prevent the separation of the cover plate from the fluted sheet, and would provide a continuous stiffening effect along the lines of connections throughout loading.

This reasoning behind the present design philosophy is well received. However, it is quite evident that the connection spac-

ing need not be made as small as that required by Eq. 1 in order for the plate buckling to take place prior to gross cylindrical buckling. Clearly, once the plate buckling initiates, it is unlikely for the separation to occur within the concave (dished-in) half buckling wave length $\lambda$, as the stress is gradually increased beyond $\sigma_{cr}$ (see Fig. 4). Furthermore, most cover plates used to form multi-cellular or single-cell panels are manufactured with overlapping edge stiffeners as illustrated in Fig. 1. Subsequent to plate buckling, but prior to yielding, such a configuration would also prevent the separation of the cover plate from the fluted sheet within the convex half of the buckling wave length. Additionally, in the case of multi-cellular panels, since the convex buckling wave is restrained by the concave buckling wave in the adjacent cell, there appears to be no reason to believe that separation of compressed plates along the lines of connections would take place.

Hence, if the connection spacing is such that the cover plate can be suppressed into the buckling configuration shown in Fig. 5, it is quite unlikely for the plate buckling to give way to gross cylindrical buckling at a value of $\sigma_c$ beyond $\sigma_{cr}$. This would provide a continuous stiffening effect along the lines of connections until the maximum edge stress $\sigma_c$ reaches the yield stress of the steel. In fact, tests conducted on composite cold-formed steel panels similar to that shown in Fig. 1 (6,9) have substantiated this observation. In light of these arguments, it appears more appropriate to base the spacing of intermittent

connections in practical cellular panels on elastic plate buckling behavior rather than on the assumption of strip column buckling.

## PROPOSED SPACING CRITERIA

There are three possible ways in which the development of the assembled member strength predicted on the basis of monolithic action may be hindered. The maximum allowable connection spacing s is the smallest value obtained by simultaneously considering the three criteria described below.

Allowable Strength of Connection. - This is a rather straightforward stipulation which simply states that the spacing, s, is not to exceed that which is required to transmit the force induced by applied loads at connections, on the basis of allowable design strength per connection. The determination of connection spacing can be based solely on this criterion when the connected components of the member are subjected to in-plane tensile stresses and the possibility of buckling does not exist. However, when the component parts are in compression, it becomes necessary to prevent the separation of compressed plates so as to preserve the validity of the assumption of fully composite action.

Separation of Compressed Cover Plates. - It is customary to design a connected section on the basis of fully composite behavior, and then detail fasteners in such a way that the desired action takes place. If the longitudinal spacing of

connections in Fig. 5 is arranged such that the continuous stiffening effect along each line of connections is ensured, the strength of each individual cell can be computed separately using effective section properties. As illustrated in App. I, the strength of the entire panel is then obtained by multiplying the strength of one cell by the number of cells in the assembly (2,9).

Below, the buckling configuration in Fig. 5 is used to develop a spacing requirement to prevent the separation of the cover plate. The elastic buckling stress of such an ideal rectangular plate compressed in one direction is given by (1);

$$\sigma_{cr} = \frac{k\pi^2 E}{12(1-\nu^2)\ (b/t)^2} \qquad (2a)$$

where E is the elastic modulus of steel, $\nu$ the Poisson's ratio, t the thickness of the cover plate, and b the width of the loaded edge of the plate. In Eq. 2a, k is usually referred to as the plate buckling stress coefficient, and for a plate simply supported on all four edges is given by;

$$k = \left(\frac{mb}{a} + \frac{n^2 a}{mb}\right)^2 \qquad (3)$$

where a is the length of plate, and the terms m and n represent the number of half-waves into which the plate buckles in the x and y directions, respectively.

Considering each cell separately, with n=1, $b = w_c$, using $\nu = 0.3$ and denoting $c = a/mw_c$ in Eq. 2a, a general expression for one half-wave length $\lambda = a/m$ (see Fig. 5), in terms of the

compressive stress $\sigma_c$, can be found. With these values, Eq. 2a becomes:

$$\sigma_c = \frac{.904E}{(w_c/t)^2} \left(\frac{1}{c} + c\right)^2 \tag{2b}$$

Solving for c from this quadratic equation yields,

$$c = \frac{a}{mw_c} = \frac{1}{2}\left\{\frac{w_c/t}{0.95}\sqrt{\frac{\sigma_c}{E}} - \sqrt{\left[\frac{w_c/t}{0.95}\sqrt{\frac{\sigma_c}{E}}\right]^2 - 2^2}\right\} \tag{5a}$$

Letting $e = (w_c/0.95t)\sqrt{\sigma_c/E}$ and $f = 2$, the square root term in Eq. 5a becomes $\sqrt{e^2-f^2} = e\sqrt{1-(f/e)^2}$. Furthermore, denoting $x = -(f/e)^2$ in this equation, and using the binomial expansion formula with only three terms yields

$$\frac{(w_c/t)}{0.95}\sqrt{\frac{\sigma_c}{E}}\left\{1 + \frac{1}{2}\left[-\left(\frac{1.9}{w_c/t}\sqrt{\frac{E}{\sigma_c}}\right)^2\right] - \frac{1}{8}\left[-\left(\frac{1.9}{w_c/t}\sqrt{\frac{E}{\sigma_c}}\right)^2\right]^2\right\}. \tag{2c}$$

Substituting Eq. 2c in place of the square root term in Eq. 5a results in

$$c = \frac{a}{mw_c} = \frac{\lambda}{w_c} = \frac{(w_c/t)}{2(0.95)}\sqrt{\frac{\sigma_c}{E}}\left[1 - 1 + \frac{1}{2}\left(\frac{1.9}{w_c/t}\sqrt{\frac{E}{\sigma_c}}\right)^2 + \frac{1}{8}\left(\frac{1.9}{w_c/t}\sqrt{\frac{E}{\sigma_c}}\right)^4\right] \tag{5b}$$

It is reasonable to assume that if the buckling configuration illustrated in Fig. 5 is to occur, at least one extra fastener should be placed within one half-wave length. Accordingly, $\lambda = 2s$ in Eq. 5b gives

$$s = 0.5t\sqrt{\frac{E}{\sigma_c}}\left[1 + \left(\frac{0.95}{w_c/t}\sqrt{\frac{E}{\sigma_c}}\right)^2\right] \tag{6}$$

Eq. 6 can further be simplified if $\sigma_{cr}$ required to initiate out-of-plane distortions in the compressed cell element of width $w_c$ is substituted for $\sigma_c$. It should be emphasized that, since the effective section properties are used in determining the ultimate flexural strength of the panel, the prevention of buckling prior to yielding is not a consideration here. The theoretical value of $\sigma_{cr}$ can be computed from Eq. 2a by using E = 29,500 ksi (203,400 MPa) and by taking k = 4 (1);

$$\sigma_{cr} = \frac{4\pi^2 E}{10.92(w_c/t)^2} = \frac{106,650}{(w_c/t)^2} \qquad (7)$$

It is noted here that the value of $\sigma_{cr}$ given by Eq. 7 is applicable only for ideal plates. In real plates, especially those in welded cold-formed steel members, the presence of inherent imperfections and residual stresses due to cold-working causes very gradual progression of stress redistribution initiated at a considerably lower stress than that indicated by Eq. 7. On the basis of his extensive investigation on cold-formed sections, Winter (5) has proposed the following semi-empirical effective width equation;

$$\frac{b_e}{w} = \sqrt{\frac{\sigma_{cr}}{\sigma_{max}}}\left(1 - 0.22\sqrt{\frac{\sigma_{cr}}{\sigma_{max}}}\right) \qquad (8)$$

where, as $\sigma_c$, $\sigma_{max}$ refers to the maximum compression edge stress, and $b_e$ is the corresponding effective width of the plate having an actual flat width of w.

With the use of Eq. 8, it becomes possible to determine the

magnitude of $\sigma_{max}$, in terms of the theoretical value of $\sigma_{cr}$, at incipient buckling in an imperfect plate. Because the entire width of the plate is effective at the initiation of buckling, $b_e = w$ in Eq. 8 results in (7,8);

$$\sigma_{max} = 0.453\ \sigma_{cr} \tag{9}$$

Then, from Eq. 7, $\sigma_{max} = \sigma_c = 0.453 \times 106{,}650/(w_c/t)^2$, or;

$$\sqrt{\sigma_c} = \frac{221}{(w_c/t)} \tag{10}$$

Substituting Eq. 10 into Eq. 6, and using E = 29,500 ksi gives,

$$s = 0.6\ w_c = 0.6\ \frac{w}{n} \tag{11}$$

where n is the number of typical cells in the panel of width w.

It is evident from Eq. 11 that as $w_c$ gets smaller, so does the spacing s between fasteners. However, if the plate is so narrow that buckling prior to yielding is not a concern, the spacing need no longer be governed by $w_c$. In order to determine a lower bound for s in such a case, the limiting value of $w_c$, $w_{lim}$, at which yielding, rather than buckling, initiates may be substituted in Eq. 11. This value of $w_{lim}$ can be found from Eq. 10 by substituting $\sigma_c = \sigma_y$;

$$w_{lim} = \frac{221t}{\sqrt{\sigma_y}} \tag{12}$$

This expression in Eq. 11 results in,

$$s = 0.6\ \left(\frac{221t}{\sqrt{\sigma_y}}\right) = \frac{133t}{\sqrt{\sigma_y}} \tag{13}$$

Hence, it is concluded that the spacing, s, in inches, in line of stress of welds, rivets, or bolts connecting a compression cover plate to another element should not exceed 0.6 times the flat width $w_c$, but need not be less than $133t\sqrt{\frac{\sigma}{y}}$.

Separation of Unstiffened Compression Plate Elements. - When the cover plate is in compression, both of the outstanding flanges of the fluted sheet would also be in compression (see Fig. 1). Such unstiffened compression elements tend to buckle at smaller stresses and into longer half-waves than corresponding stiffened plates. The buckling configuration of a compressed unstiffened plate is illustrated in Fig. 6.

For an elastically restrained unstiffened compression element, the coefficient k in Eq. 2a is given as (1);

$$k = \left(\frac{m}{\alpha}\right)^2 + p + q \cdot \left(\frac{\alpha}{m}\right)^2 \qquad (14)$$

where $\alpha$ is the aspect ratio a/b. The factors p and q depend on the coefficient of elastic restraint $\beta$ provided by the supported unloaded edge. The value of $\beta$ is directly proportional to the angle of rotation of the restraining plate, i.e., of the web element. Accordingly, $\beta = 0$ indicates an infinitely rigid web element (fixed edge), and $\beta = \infty$, an infinitely flexible web element indicating no restraint against rotation (simply supported edge). For $\beta > 1.6$, the values of p and q can be computed using

$$p = .425 + \frac{.016}{.025+\beta} \quad , \qquad (15)$$

and

$$q = \frac{.061}{.43+\beta} \tag{16}$$

The value of the aspect ratio $\alpha_0$ for which $\sigma_{cr}$ reaches a minimum is found by substituting Eq. 14 into Eq. 2a, and using the condition that $\partial\sigma_{cr}/\partial\alpha = 0$. This gives (1),

$$\alpha_0 = \frac{a}{b} = \frac{m}{\sqrt[4]{q}} \tag{17}$$

Using Eq. 17 in Eq. 14 results in;

$$k = p + 2\sqrt{q} \tag{18}$$

Eq. 17 can be used to determine the length of a half buckling wave of an unstiffened plate having a width of $b = w_u$;

$$\lambda = \frac{a}{m} = \frac{w_u}{\sqrt[4]{q}} \tag{19}$$

where q is to be determined from Eq. 16 for an appropriately specified coefficient of restraint $\beta$. In Ref. 1, excluding initial imperfections and assuming straight edges prior to local buckling, approximate formulas for the coefficient of restraint for the webs and flanges of a number of practical sections are derived. Such assumptions are clearly not realistic for cold-formed steel sections which inherently possess pronounced initial imperfections.

In Table 1, values of k and $\lambda$ are computed for several specified values of $\beta$, using Eqs. 18 and 19, respectively. The plate buckling coefficient k is plotted against the coefficient of elastic restraint $\beta$ in Fig 7. It is evident from Fig. 7 that the coefficient k becomes quite insensitive for large values of

$\beta$, especially beyond $\beta = 5{,}000$. The value of $k = .425$ corresponds to cases in which no restraint against rotation is provided by the web, i.e., $\beta = \infty$. This value can be computed by using Eqs. 15 and 16 in Eq. 18.

Quite obviously, the amount of web restraint in cold-formed steel members cannot be generalized, but would appear to depend on the shape, thickness, and the manufacturing process. Hence, an experimental investigation may be the best means of determining realistic values of $\beta$. In the absence of experimental data, based on the assumption that a small amount of rotational restraint corresponding to $\beta = 5{,}000$ and $k = .432$ is provided by the web element, the half buckling wave length is $\lambda = 17\, w_u$ (see Table 1). Again, placing one extra connection within the length $\lambda$ yields,

$$s = 8w_u \tag{20}$$

When the unstiffened element is not slender and buckling is of no concern, the spacing need not be controlled by $w_u$ as indicated by Eq. 20. As in the case of stiffened flanges, in order to determine a lower bound for connection spacing, the limiting value of the unstiffened flange width $w_u$ can be substituted into Eq. 20. Noting that, at present, the design of unstiffened compression elements is not based on post-buckling strength, the value of $(w_u)_{lim}$, for which the allowable stress is $0.6 \times \sigma_y$, is given as $63.3t/\sqrt{\sigma_y}$, in Fig. C.17 of Ref. 5 . Thus, Eq. 15 gives,

$$s = 8 \times \frac{63.3t}{\sqrt{\sigma_y}} = \frac{507t}{\sqrt{\sigma_y}} \tag{21}$$

It is then concluded that, in order to provide a continuous stiffening effect along the lines of connections joining unstiffened compression elements, the spacing of joints in an assembly should comply with the requirement that s not be larger than that obtained from Eq. 20, but it need not be smaller than the value given by Eq. 21.

## COMPARISON WITH TESTS

In Ref. 9, full-scale tests conducted on closed cellular panels with riveted and welded connections are reported. In order to determine the characteristics and strength of the fasteners used in actual assemblies, single lap joint shear tests were performed on several different steel gage combinations. In shear tests, slip load and ultimate load per connection were determined. Full-scale panel tests were carried out on single and multiple span specimens with the primary purpose of substantiating the conservative nature of the AISI provisions. In order to simulate practical usage, flat cover plates with and without perforation were used. Furthermore, in some tests a wire mesh was placed between the fluted and flat sheets.

The relevant information and the test data concerning the single span beam specimens and the two and three equal-span continuous beam specimens are presented in Table 2 and 3, respectively. All specimens were subjected to simulated uniform loading. In the preliminary simple beam specimens, fasteners were spaced in accordance with the connection strength criterion, but

the AISI buckling provisions were disregarded even when the cover plates were in compression. These preliminary tests resulted in the experimental determination of the limiting value of rivet spacing, $s_{lim}$. The value of $s_{lim}$ = 15 in. (38 cm) was chosen such that even for the most critical gage combinations considered, the limited separation of compressed plates along the lines of connections did not interfere with the development of the predicted strength of the assembly.

The description of the single panel specimens with riveted connections is given in columns 1 through 5 of Table 2. The spacing of connections in single span specimens was computed on the basis of either ultimate load or slip load obtained in shear tests. The values of s listed in column 6 of Table 2 were used in tests and are all based on the ultimate connection strength, with the exception of Specimen S7. Comparisons of specimens S7 and S8 reveals the fact that the spacing based on strength is reduced considerably when no slippage at connections is allowed. For comparison, the rivet spacings computed in accordance with the present AISI provisions and the proposed requirements are listed in columns 7 and 8, respectively. The predicted total load carrying capacity of each assembly is listed in column 9. The experimental values of the failure load are given in column 10. Simple beam specimens S9 through S12 were tested so that the cover plate was in compression.

The types of connections used in multispan beam specimens are indicated in Column 7 of Table 3. The values of s based on

connection strength, on the AISI provisions, and on the proposed requirements are listed in columns 8, 9, and 10, respectively. In regard to continuous flexural panels, a cover plate in compression in the negative moment region will be in tension in the positive moment region. Hence, all three spacing criteria should be simultaneously considered. In Appendix I, the calculation of panel strength and maximum deflection is illustrated for a two-span specimen. Furthermore, connection spacing used in tests and those based on the present and proposed criteria are determined, and additional comments are provided.

All specimens listed in Tables 2 and 3 carried loads in excess of their predicted capacities, with the exception of Specimen S12, which carried 96.5% of its theoretical yield load. Since the ultimate connection strength criterion had resulted in an excessively large rivet spacing for Specimen S12 (s = 23 in. (58.5 cm)), the premature failure of the assembly was attributed to the excessive separation of the cover plate, which apparently caused the termination of composite action. Clearly, however, the fact that such large spacings based on connection strength permitted the development of full flexural capacity in tests raises valid questions as to the conservative nature of the present AISI provisions.

## SUMMARY AND CONCLUSIONS

Based on elastic plate buckling theory, design criteria for intermittent connection spacing in cold-formed steel cellular

panels under flexural loading are developed. The proposed requirements are simple and suitable for direct use in practical design. The provisions in the current AISI Specification are reviewed. The proposed requirements and the AISI provisions are compared with the available test data. This comparison has revealed that, even though the proposed requirements result in larger values for maximum connection spacing than those obtained using the current AISI provisions, they appear to be considerably conservative when compared with the test results.

It should be noted, however, that while the proposed criteria are developed on the premise that no separation between the compressed cover plate and fluted sheet takes place, the maximum spacing used in experiments was based on connection strength. As a consequence, separation of component plates between adjacent connections were observed in tests. Apparently, this behavior did not hinder the development of the full flexural capacity of the specimen predicted on the basis of effective section properties using well established analytical procedures. On the other hand, deflections observed in tests were considerably larger than the corresponding predicted values. This loss in stiffness of the assembly is attributed to the separation of the compression elements along the lines of connections, regardless of the connection type used, and, in addition, to slippage in the case of riveted connections.

Accordingly, it is apparent that connection spacing may be chosen in such a way that either (a) the fully composite action

of the assembly, in regard to both strength and deflection, takes place, or (b) only the full development of the predicted flexural capacity is sufficient, when relatively large deflections are tolerable (9). The criteria developed here is in compliance with the former requirement.

## APPENDIX I. - TWO EQUAL-SPAN CELLULAR PANEL WITH PERFORATED COVER PLATE

The information listed in Table 4, regarding the two equal-span, uniformly loaded test specimens C5 through C8, is taken from Refs. 4 and 9. The panel geometry and tested cover plate down configuration, along with the centerline dimensions of a typical cell, are shown in Fig. 8. It is required that (a) maximum load carrying capacity, (b) required connection spacing, and (c) maximum deflection at yield be computed.

The following general expressions can be derived to determine the elastic section properties of a typical cell. The cross-sectional properties of thin-walled shapes can be computed on the basis of line elements using centerline dimensions which can then be multiplied by respective thicknesses. The radius of corner bends can be neglected without any appreciable error (8).

Location of Neutral Axis. - From the top flange designated as $b_f$ in Fig. 9a;

$$y_n = \frac{t_f(b_r+d_w)d_f+t_p b_p d_p}{t_f(b_f+b_r+2d_w)+t_p b_p} \qquad (22)$$

In Eq. 22, where appropriate, corresponding effective widths

should be used for $b_f$, $b_r$ or $b_p$.

Moment of Inertia of Panel. - From Fig. 9b, the moment of inertia of an inclined web about the u-axis, $I_{wu}$, is

$$I_{wu} = I_{wx} \cos^2\theta = (\frac{1}{12} t_f d_w^3) \frac{d_f^2}{d_w^2} = \frac{1}{12} t_f d_w d_f^2 \quad (23)$$

Then, the moment of inertia of the inclined web with respect to the neutral axis (NA) of the cell, $I_{wn}$, becomes

$$I_{wn} = I_{wu} + A_w (\frac{d_f}{2} - y_n)^2 \quad (24)$$

where $A_w$ is the area of one web element.

Using Eq. 24, the moment of inertia of a typical cell with respect to the NA can now be derived as

$$I_c = t_f\{b_f y_n^2 + 2d_w[\frac{d_f^2}{12} + (\frac{d_f}{2} - y_n)^2] + b_r(d_f - y_n)^2\} + t_p b_p (d_p - y_n)^2 \quad (25)$$

Considering that there are three typical cells in the panel, the moment of inertia of the panel becomes $I_p = 3I_c$ (2). Accordingly, the yield moment of the assembly can be found from

$$M_y = \frac{\sigma_y I_p}{y_y} \quad (26)$$

where $y_y$ refers to the distance from the NA to the flange where yielding initiates.

(a) Determination of Yield Load

Since the yield moment capacity in the positive and the negative bending moment regions, i.e., $M_y^+$ and $M_y^-$ respectively, are usually different in such members, the elastic moment diagram

(Fig. 10c) alone is not sufficient to determine the location of initial yielding. The $(M_y^+/M_y^-)$ ratio should also be considered.

Positive Bending Moment Region (+BMR). - In this region, $b_f$ is in compression, while $b_r$ and $b_p$ are in tension. The flat-width ratio of the compression flange is

$$\frac{b_f}{t_f} = \frac{6.865}{.0515} = 133.3 = \frac{965}{\sqrt{\sigma_y}} > \frac{221}{\sqrt{\sigma_y}}$$

where $221/\sqrt{\sigma_y}$ is the limiting flat-width ratio given by Eq. 12. Hence, the compression flange is partially ineffective. The effective width equation, Eq. 8, can also be written as (5)

$$b_e = 1.9t\sqrt{\frac{E}{\sigma_{max}}}\left(1 - \frac{.415}{w/t}\sqrt{\frac{E}{\sigma_{max}}}\right) \qquad (27)$$

Assuming that yielding initiates in the compression flange, Eq. 27 can now be used to determine the effective width of the compression flange, $b_{fe}$, at $\sigma_{max} = \sigma_y$. As specified in Table 4, using E = 29,650 ksi (204,289 MPa) and $t = t_f$ = .0515 in. (1.3 mm) results in $b_{fe}$ = 2.155 in. (5.5 cm).

It is indicated in Ref. 6 that 25% perforation corresponds to 50% reduction in the cover plate, with the effective $b_p$ being 7.803/2 = 3.9015 in. (9.91 cm). Hence, the effective cross-section for stress calculations in the +BMR becomes as shown in Fig. 11. Using Eq. 22 with $b_f = b_{fe}$, the NA can be located at $y_n = y_c$ = .900 in., where $y_c$ indicates the distance from the NA to the compression flange. Then, the distance to the outermost tension flange is $y_t$ = .665 in. (1.69 cm). Hence, yielding does initiate in the compression flange.

The moment of inertia of the typical cell shown in Fig. 11 can now be computed using Eq. 25 as $I_c^+ = .204$ in.$^4$ (8.5 cm$^4$). Considering $I_p^+ = 3I_c^+ = .612$ in.$^4$ (25.5 cm$^4$) and using Eq. 26 gives the yield moment capacity for sections in the +BMR as $M_y^+ = 35.64$ in-k = 2970.0 ft-lbs. (4,028.4 m-N). Using the relationship $.0703\ w_y^+ L^2 = M_y^+$ in Fig. 10c, the uniform load inducing yielding in this region can be found as $w_y^+ = 862.2$ lbs/ft (12.6 kN/m).

Negative Bending Moment Region (-BMR). - In this region, $b_p$ and $b_r$ are in compression while $b_f$ is in tension. Since $b_r/t_f = 9.7 = 70/\sqrt{\sigma_y} < 221/\sqrt{\sigma_y}$, $b_r$ is fully effective. However, the flat-width ratio of the cover plate is $b_p/t_p = 3.9015/.041 = 95.2 = 689/\sqrt{\sigma_y} > 221/\sqrt{\sigma_y}$. This indicates that, in addition to perforation, the cover plate width should be further reduced. Again, assuming that yielding initiates in the compression flange, $b_p$, the effective width $b_{pe}$ at $\sigma_{max} = \sigma_y$ can be found using Eq. 27 as 1.661 in. (4.2 cm). The corresponding effective cross section of a typical cell in the -BMR is shown in Fig. 12. Using Eq. 22 with $b_p = b_{pe} = 1.661$ in. gives $y_n = .439$ in. (1.1 cm). In this region, $y_n = y_t = .439$ in. with $y_c = 1.126$ in. (2.9 cm). This indicates that yielding initiates in the compression flange as assumed.

Following the same procedure as in +BMR, $I_c^- = .231$ in.$^4$ (9.6 cm$^4$), $I_p^- = 3I_c^- = .6935$ in.$^4$ (28.8 cm$^4$) and $M_y^- = 32.3$ in-k = 2,690 ft-lbs (3651 m-N). Using the relationship $.125\ w_y^- L^2 = M_y^-$ in Fig. 10c, the linear load corresponding to yielding in the -BMR is $w_y^-$ = 440 lbs/ft (6.4 kN/m). Comparing $w_y^+$ and $w_y^-$, it can be

concluded that yielding originates in the -BMR at $w_y$ = 440 lbs/ft. The equivalent uniform surface load over one panel is 226 lbs/ft$^2$ (10.8 kPa) (see Table 3).

(b) Maximum Connection Spacing

Based on Strength. - From Fig. 10b, the maximum shear force is $V_{max}$ = .625 wL = .625 x 440 x 7 = 1925 lbs (8.5 kN). Adopting the simple beam theory, the shear flow at the corresponding section at the level of connections is

$$q = \frac{V_{max}Q}{I} = \frac{1925(3x1.661x.041x1.126)}{.6935} = 638.6 \text{ lbs/in } (11.2N/m)$$

Hence, shear force per line of connections is q/4 = 159.64 lbs/in. As indicated in Table 4, each rivet is capable of resisting an ultimate shear force of $V_u$ = 1700 lbs. Thus, the maximum spacing can be determined from the relationship 159.64 s = 1700 as s = 11.0 in (28 cm). It should be noted that the values s = 12 in. (30.5 cm) and s = 6 in. were used in two span beam tests solely to compare the behaviors of panels with equally spaced welded and riveted connections.

Since the spacing of connections in compression regions are also of interest here, other requirements regarding the separation of compressed plates should also be considered.

Based on AISI Requirements. - From Eq. 1, s = 259x.041/ $\sqrt{52.4}$ = 1.5 in. (3.8 cm). Additionally, regarding outstanding flanges, s = 3x0.5 = 1.5 in. (>190x.0515/ $\sqrt{52.4}$ = 1.4 in.). Hence, s = 1.5 in. controls the spacing (see Table 3).

Based on Proposed Requirements. - From Eqs. 11 and 13, s = .6x7.803 = 5.0 in (>133x.041/$\sqrt{52.4}$ = .8 in.). Regarding the unstiffened flanges, using Eqs. 20 and 21 give s = 8x0.5 = 4.0 in (>507x.0515/$\sqrt{52.4}$ = 3.6 in). Hence, s = 5.0 in. (12.7 cm) can be used for the inner lines, while s = 4.0 in (10.2 cm) for the outer lines of connections. For practical purposes, however, it is common to use the same spacing along outer and inner lines of connections (see Table 3).

(c) Maximum Deflection at Yield

For a uniformly loaded two equal-span continuous beam having a uniform moment of inertia I, the maximum deflection, at a distance .4215L from outside supports, is given by ( 7)

$$\delta_m = \frac{wL^4}{185EI} \qquad (28)$$

For cold-formed steel continuous members where the effective section properties vary from one section to the other along the beam, the average of $I^+$ and $I^-$, which are the minimum moment of inertia within the +BMR and -BMR, respectively, can be used in deflection calculations (3,5). $I^-$ is $I_y^- = .6935$ in$^4$ (28.9 cm$^4$) as computed before at yield. However, to determine the effective section properties in the +BMR, thus $I^+$ at failure, a trial-and-error procedure should be employed.

The static value of the maximum positive bending moment at yield, from Fig. 10c, is $M_{st}^+ = .0703x440x7^2 = 1453.8$ ft-lbs = 17.45 in-k (1972.4 m-N). The correct value of $\sigma_c$ corresponding to this bending moment can be found by first assuming a value for

$\sigma_c$. Then, effective section properties can be determined using Eqs. 22 and 25, and the resisting moment $M_r^+$ can be computed using Eq. 26. This procedure can be repeated until $M_r^+$ is approximately equal to $M_{st}^+$, with the corresponding moment of inertia being $I^+$.

Assuming $\sigma_c$ = 19 ksi (131 MPa) and referring to Fig. 11 gives $b_{fe}$ = 3.39 in. (8.6 cm). And, following the previously adopted procedure, $y_n = y_c$ = .79 in (2 cm), and $I_c^+$=.2493 $in^4$ (10.4 $cm^4$). With $I_p^+ = 3I_c^+$ = .748 $in^4$, $M_r^+$ = 17.99 in-k (2033.4 m-N) which is sufficiently close to $M_{st}^+$. Hence, $I^+$ = .748 $in^4$ can be taken without any appreciable error. Then, the average moment of inertia is (.748 + .6935)/2 = .721 $in^4$ (30 $cm^4$). Now, using Eq. 28 gives

$$\delta_m = \frac{(440/12,000)x84^4}{185x29,650x.721} = .46 \text{ in. } (1.2 \text{ cm})$$

The experimentally measured average value of $\delta_m$ at approximately 440 lbs/ft (6.4 kN/m) is 0.65 in. (1.7 cm). The large discrepancy between the predicted and experimental values becomes quite evident when it is considered that, in tests, large values of s were used permitting considerable separation of compressed plates. Furthermore, additional loss in stiffness would have occurred due to slippage at rivets. In Ref. 9, an empirical method of predicting design deflections accounting for separation and slippage is described.

APPENDIX II. - REFERENCES

1. Bleich, F., Buckling Strength of Metal Structures, McGraw-Hill Book Company, Inc., New York, 1952.

2. Rockey, K. C., and Hill, H. V. (editors), Thin Walled Steel Structures - Their Design and Use in Buildings, Crosby Lockwood and Sons, Ltd., London, 1969, p. 236.

3. Specifications for the Design of Cold-Formed Steel Structural Members, American Iron and Steel Institute, Washington, D.C., 1983.

4. White, R. N., and Yener, M., "Provisions for the Design of Walcon Corporation 24 in. NDU Panels with Riveted Connections", Walcon Corporation, Ecorse, MI, February 1981.

5. Winter, G., Commentary on the 1968 Edition of the AISI Specifications, American Iron and Steel Institute, New York, N.Y., 1970.

6. Yener, M., and White, R. N., "Progress Reports on Walcon Corporation 24" NDU Panels, R1 through R8", Department of Structural Engineering, Hollister Hall, Cornell University, Ithaca, N.Y., 1978-1980.

7. Yener, M., "Maximum Allowable Spacing of Intermittent Connections in Cold-Formed Steel Members", Structural Engrg., Report No. CE-STR-82-22, Purdue Univ. West Lafayette, IN, 1982.

8. Yener, M., and Pekoz, T., "Limit Design in Cold-Formed Steel", ASCE, J. of Struct. Div., Vol. 109, No. 9, September, 1983.

9. Yener, M., and White, R. N., "Cold-Formed Steel Panels with Riveted Connections", ASCE, J. of Struct. Div., Vol. 110, No. 5, May 1984.

APPENDIX III. - NOTATIONS

The following symbols are used in this paper;

| | |
|---|---|
| $A_w$ | = area of one web element; |
| a | = length of half-buckling-waves; |
| b | = width of the loaded plate edge; |
| $b_e$ | = effective width of compression elements; |
| $b_f$, $b_p$, $b_r$ | = widths of elements as defined in Fig. 8a; |
| $b_{fe}$, $b_{pe}$ | = effective widths of flanges $b_f$ and $b_p$ (Fig. 8a), respectively, when in compression; |
| $d_f$, $d_p$, $d_w$ | = depths of flange and web elements as defined in Fig. 8a; |
| E | = modulus of elasticity; |
| f | = design stress, $0.6\sigma_y$; |
| $I_p$ | = moment of inertia of the panel; |
| $I_c$ | = moment of inertia of a typical cell; |
| $I_{wn}$, $I_{wu}$, $I_{wx}$ | = moment of inertia of inclined web with respect to the neutral, u , and x axes; |
| k | = plate buckling stress coefficient; |

$L$ = length of span;

$M_y^+$ $M_y^-$ = yield moment in the positive and negative bending moment regions;

$m$ = number of half-waves in the direction of stress;

$n$ = number of half-waves in the transverse direction, and number of typical cells in the assembly;

$p$, $q$ = coefficients in Eq. 14;

$q$ = shear flow at the level of connections;

$r$ = radius of gyration;

$s$ = center-to-center spacing between fasteners in line of stress;

$s_{lim}$ = maximum allowable s in members designed for strength;

$t_f$, $t_p$ = thickness of material as defined in Fig. 8a;

$V_u$ = ultimate shear force capacity per connection;

$w$ = center-to-center distance between the outer line of fasteners;

$w_c$ = flat width of a typical cell;

$w_{lim}$ = limiting flat width for fully effective sections;

$w_p$ = total width of the cover plate;

$w_u$ = flat width of outstanding flanges;

$w_y$ = uniform yield load;

$y_c$ = distance from neutral axis to compression flange;

$y_n$ = distance from neutral axis to top flange;

$y_y$ = distance from neutral axis to yielded flange;

$\alpha$ = aspect ratio, a/b;

$\beta$ = coefficient of elastic restraint;

$\delta_m$ = maximum panel deflection;

$\theta$ = angle as defined in Fig. 8b;

$\lambda$ = half buckling wave length, a/m;

$\nu$ = Poisson's ratio;

$\sigma_c$, $\sigma_{max}$ = maximum compression edge stress;

$\sigma_{cr}$ = elastic plate buckling stress; and

$\sigma_y$ = yield stress of the material.

Table 1. - Determination of the $\lambda/w_u$ Ratio for Specified Values of $\beta$.

| $\beta$ | $px10^3$ (Eq. 15) | $qx10^6$ (Eq. 16) | k (Eq. 18) | $\lambda/w_u$ (Eq. 19) |
|---|---|---|---|---|
| 100 | 425.160 | 607.39 | .475 | 6.4 |
| 200 | 425.080 | 304.35 | .460 | 7.6 |
| 400 | 425.040 | 152.34 | .450 | 9.0 |
| 1000 | 425.016 | 60.97 | .441 | 12.0 |
| 2000 | 425.008 | 30.49 | .436 | 13.5 |
| 3000 | 425.005 | 20.33 | .434 | 15.0 |
| 5000 | 425.003 | 12.20 | .432 | 17.0 |
| 7000 | 425.002 | 8.71 | .431 | 18.4 |
| 9000 | 425.002 | 6.78 | .430 | 19.6 |
| 10000 | 425.002 | 6.10 | .430 | 20.0 |

TABLE 2. - Simple Span Beams with Riveted Connections

| Specimen No. (1) | Sheet Gage (Flat-Fluted) (2) | Wire Gage (3) | % Perf. (4) | Position of Cover Plate (5) | s, in. (strength) (6)[a] | s, in. (AISI) (7) | s, in. (Proposed) (8) | $P_y$, lbs. (Predicted) (9) | $P_u$, lbs. (Experimental) (10) |
|---|---|---|---|---|---|---|---|---|---|
| S2 | 18-18 | - | - | Down | 10.0 | 10.0 | 10.0 | 2136 | 2658 |
| S4 | 18-18 | 17 | - | Down | 9.5 | 9.5 | 9.5 | 2136 | 2473 |
| S6 | 18-18 | - | 25 | Down | 12.5 | 12.5 | 12.5 | 2044 | 2288 |
| S7 | 22-22 | - | - | Down | 5.5[b] | 5.5 | 5.5 | 1207 | 1278 |
| S8 | 22-22 | - | - | Down | 14.0 | 14.0 | 14.0 | 1207 | 1338 |
| S9 | 18-18 | - | - | Up | 12.0 | 1.5 | 4.0 | 2648 | 2700 |
| S10 | 18-18 | 17 | - | Up | 11.0 | 1.5 | 4.0 | 2658 | 2822 |
| S11 | 18-18 | - | 25 | Up | 13.0 | 1.5 | 4.0 | 2535 | 2682 |
| S12 | 22-22 | - | - | Up | 23.0 | 1.3 | 4.0 | 1442 | 1392 |

[a] Spacings of the test specimens based on ultimate connection strength.

[b] Based on average slip shear load.

Note: 1 in. = 2.54 cm, 1 lb. = 4.45 N.

TABLE 3. - Multiple Span Beams

| Specimen No. (1) | No. of Spans (2) | Sheet Gage (Flat-Fluted) (3) | Wire Gage (4) | % Perf. (5) | Position of Cover Plate (6) | Type of Connection (7) | s, in. (strength) (8)[a] | s, in. (AISI) (9) | s, in. (Proposed) (10) | $P_y$, psf. (Predicted) (11) | $P_u$, psf. (Experimental) (12) |
|---|---|---|---|---|---|---|---|---|---|---|---|
| C1 | 3 | 18-18 | 17 | - | Up | Riveted | 4.5 | 1.5 | 4.0 | 249 | 313 |
| C2 | 3 | 18-18 | - | - | Up | Riveted | 5.0 | 1.5 | 4.0 | 238 | 269 |
| C3 | 3 | 18-18 | - | - | Down | Riveted | 7.0 | 1.5 | 4.0 | 265 | 287 |
| C4 | 3 | 22-22 | - | - | Down | Riveted | 13.0 | 1.3 | 4.0 | 144 | 145 |
| C5 | 2 | 20-18 | - | 25 | Down | Riveted | 12.0 | 1.5 | 4.0 | 226 | 289 |
| C6 | 2 | 20-18 | - | 25 | Down | Welded | 12.0 | 1.5 | 4.0 | 226 | 267 |
| C7 | 2 | 20-18 | - | 25 | Down | Riveted | 6.0 | 1.5 | 4.0 | 226 | 270 |
| C8 | 2 | 20-18 | - | 25 | Down | Welded | 6.0 | 1.5 | 4.0 | 226 | 287 |

[a] Spacings of the test specimens.

Note: 1 in. = 2.54 cm, 1 psf = 47.9 Pa.

Table 4. - Properties of Two-Equal Span Test Panels

| | Position | Gage | % Perforation | t(in) | $\sigma_y$(ksi) |
|---|---|---|---|---|---|
| Fluted Sheet | up | 18 | none | .0515 | 52.4 |
| Cover Plate | down | 20 | 25 | .0410 | 52.4 |

Note: $V_u$, ultimate shear strength per connection = 1,700 lbs (7565 N)

E = 29,650 ksi (204 289 MPa)

1 in. = 2.54 cm, 1 ksi = 6.89 MPa

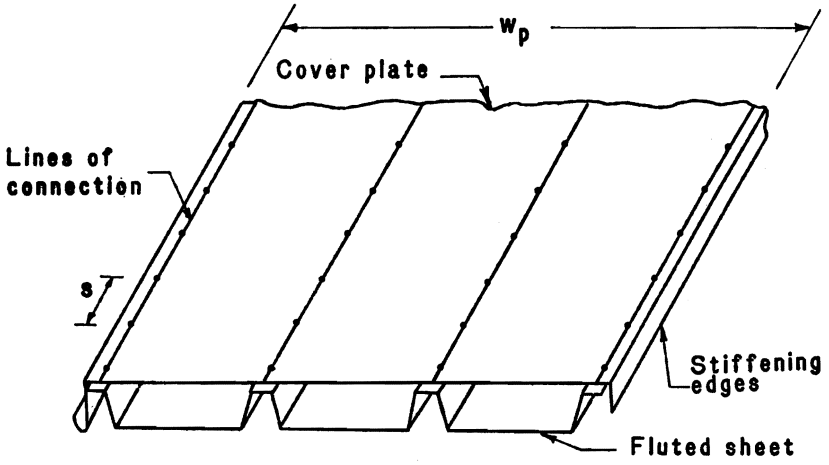


Fig. 1. – Cellular Panel with Flat Cover Plate

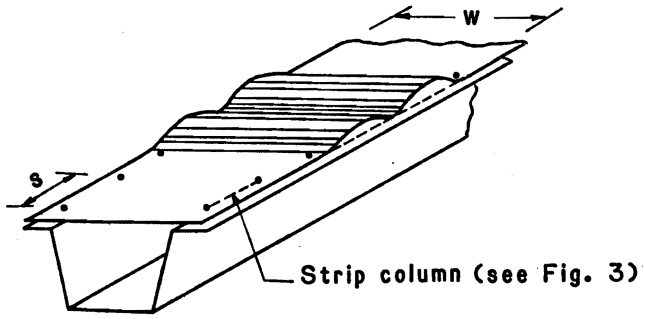


Fig. 2. – Cylindrical Buckling of Cover Plate

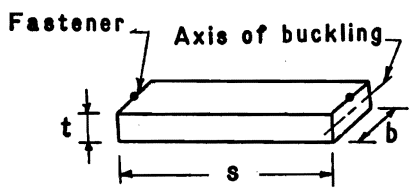


$$r = \sqrt{\frac{I}{A}}$$

$$= \sqrt{\frac{1}{12} bt^3 / bt} = \frac{t}{\sqrt{12}}$$

Fig. 3. – Radius of Gyration for Strip Column Between Fasteners

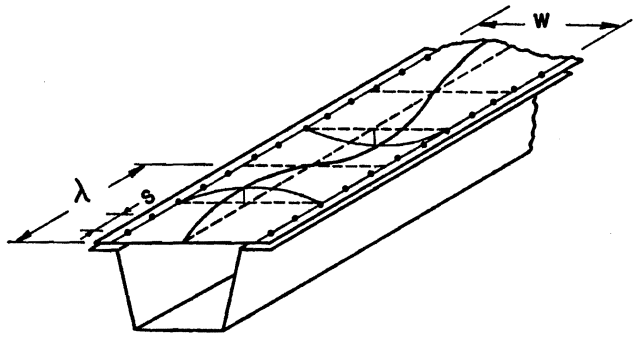


Fig. 4. – Plate Buckling of Cover Sheet

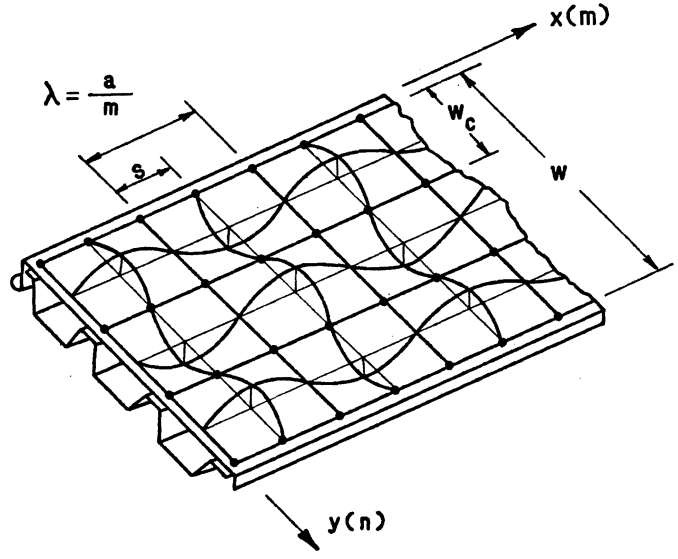


Fig. 5. – Buckling Configuration of Cover Plate With Adequate Connection Spacing

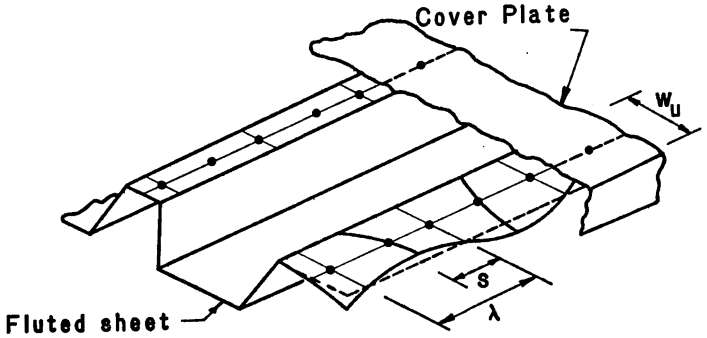


Fig. 6. – Buckling of Outstanding Unstiffened Flanges

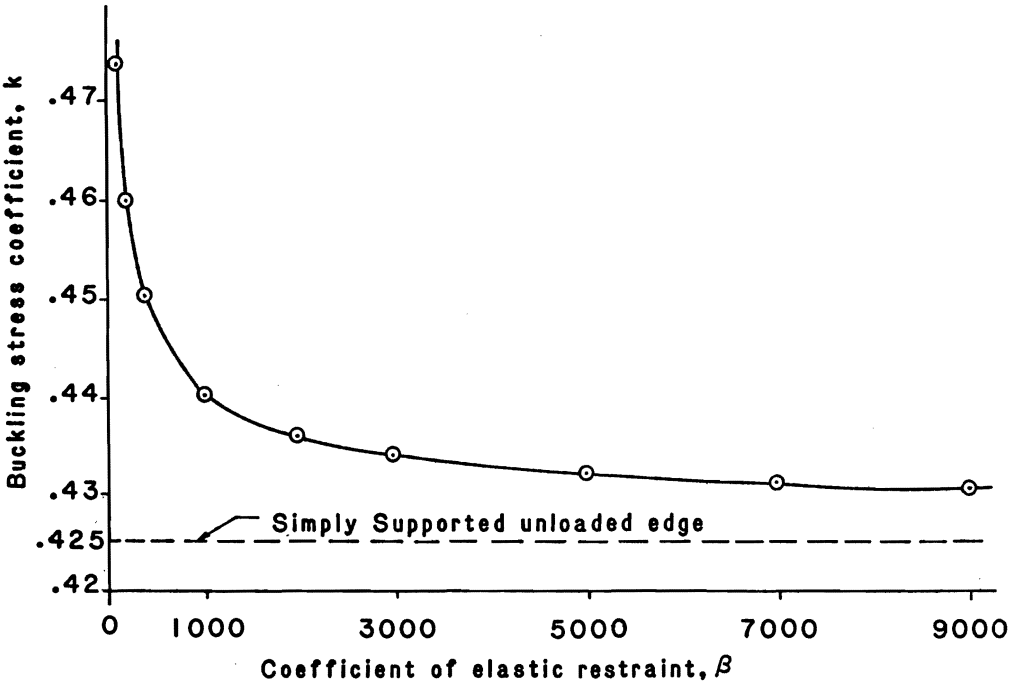


Fig. 7. – variation of Coefficient k with Edge Restraint

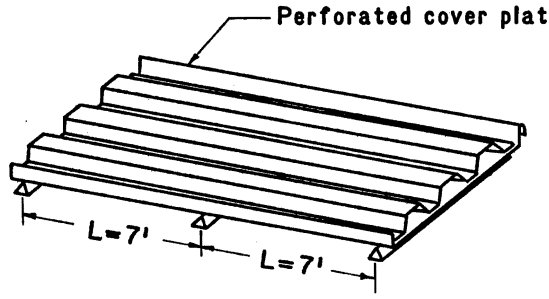


(a) Panel in Tested Configuration

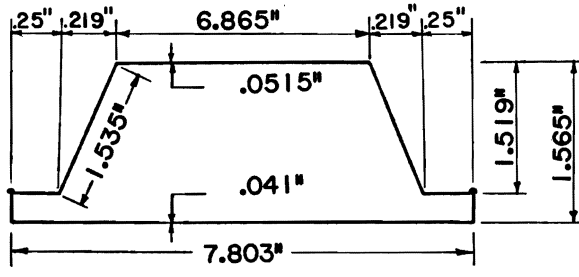


(b) Center–Line Dimensions of a Typical Cell

Fig. 8. – Two Equal Span Panel Geometry

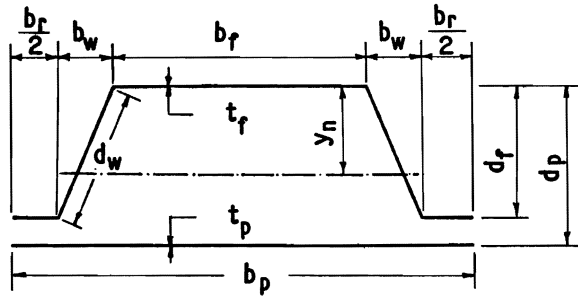


(a) Typical Cell Description

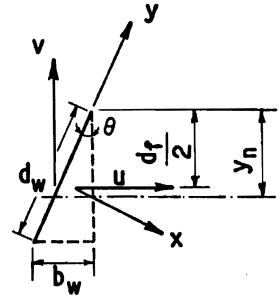


(b) Inclined Web Element

Fig. 9. – Notation Used In App. I

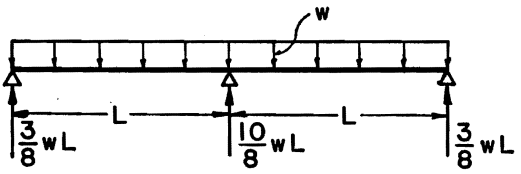


(a) Loading and Reactions

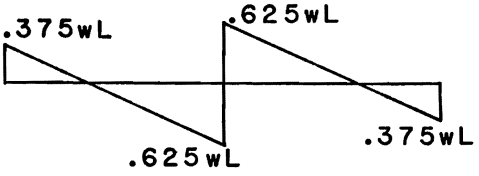


(b) Shear Distribution

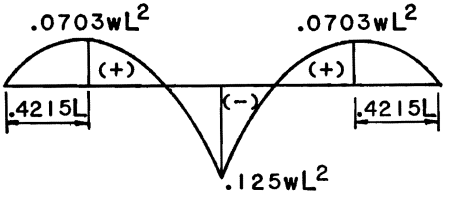


(c) Moment Distribution

Fig. 10. – Two Equal–Span Continuous Beam

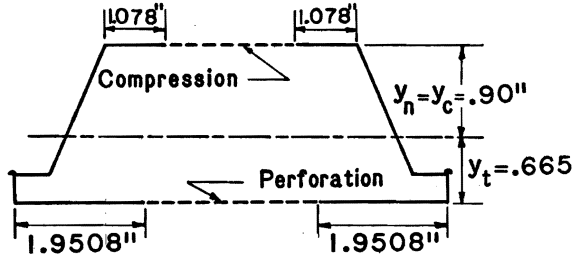


Fig. 11. – Effective Section Properties in +BMR

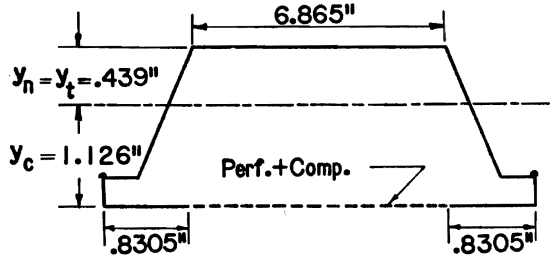


Fig. 12. – Effective Section Properties in –BMR